JOURNAL OF SPACECRAFT AND ROCKETS
Vol. 47, No. 6, November–December 2010

Asteroid Destinations Accessible for Human Exploration: A Preliminary Survey in Mid-2009

Daniel R. Adamo*
Houston, Texas 77059
Jon D. Giorgini†
Jet Propulsion Laboratory, California Institute of Technology, Pasadena, California 91109-8099
and
Paul A. Abell‡ and Rob R. Landis§
NASA Johnson Space Center, Houston, Texas 77058

DOI: 10.2514/1.48681

The flexible path is one of several space exploration strategy options developed by the Review of U.S. Human Space Flight Plans Committee in 2009. Among proposed flexible path destinations are near-Earth objects, those asteroids and comets having perihelions of less than 1.3 astronomical units and periods of less than 200 years. Heliocentric-orbit element criteria have been developed with the objective of rapidly identifying the near-Earth object subset potentially accessible for human exploration capabilities. When these criteria were applied to the Jet Propulsion Laboratory's small-body database in June 2009, the accessible subset was found to contain 36 near-Earth objects. Opportunities to visit these destinations have been obtained and assessed over the interval from 2020 through 2050. With the number of cataloged near-Earth objects expected to grow by more than an order of magnitude in the next 20 years, the number and frequency of human near-Earth object exploration opportunities will likewise increase.

Nomenclature

a = near-Earth object heliocentric-orbit semimajor axis, astronomical units
a_A = maximum heliocentric semimajor axis of a spacecraft Earth departure trajectory with energy $C3_X$, km or astronomical units
a_P = minimum heliocentric semimajor axis of a spacecraft Earth departure trajectory with energy $C3_X$, km or astronomical units
$C3$ = spacecraft geocentric Earth departure energy (equivalent to v_{HE}^2), $\mathrm{km}^2/\mathrm{s}^2$
$C3_X$ = maximum $C3$ launch-vehicle capability for a spacecraft of minimum mass (45.2 mT)
e = near-Earth object heliocentric-orbit eccentricity
e_A = eccentricity of a spacecraft heliocentric elliptical orbit with apses $r_A \times r_M$
e_P = eccentricity of a spacecraft heliocentric elliptical orbit with apses $r_M \times r_P$
I_{SP} = propulsive specific impulse, s
i = near-Earth object heliocentric-orbit inclination on the epoch J2000.0 ecliptic plane, deg
i_X = spacecraft maximum attainable i after $C3_X$ is depleted by Δv, deg
p = near-Earth object heliocentric-orbit semilatus rectum, km or astronomical units
r_A = aphelion distance of a spacecraft Earth departure trajectory with semimajor axis a_A, km or astronomical units
r_{EPO} = geocentric radius of a circular Earth parking orbit, km
r_M = spacecraft reference heliocentric distance at Earth departure (1 astronomical unit or 149,597,870.691 km) [3]
r_{MIN} = nominal (best-estimate) near-Earth object minimum geocentric distance during an encounter with Earth, astronomical units
r_P = perihelion distance of an Earth departure trajectory with semimajor axis a_P, km or astronomical units
v_E = spacecraft heliocentric speed in the ecliptic plane at Earth departure, km/s
v_{EI} = geocentric spacecraft return trajectory speed at 121.92 km height (approximate entry interface) above a spherical Earth of radius 6378.136 km [3], km/s
v_{HE} = geocentric spacecraft asymptotic hyperbolic excess speed as Earth's gravitational sphere of influence is departed, km/s
v_M = heliocentric spacecraft orbit speed at r_M, km/s
v_{MIN} = near-Earth object geocentric speed at the r_{MIN} encounter epoch, km/s
v_R = near-Earth object heliocentric radial velocity component at heliocentric distance r_M, km/s
v_T = near-Earth object heliocentric tangential velocity component at heliocentric distance r_M, km/s
ΔT = spacecraft round-trip mission duration, days
Δv = heliocentric velocity difference magnitude between a near-Earth object crossing a circular orbit of radius r_M and motion in the circular orbit at the crossing point, km/s
Δv_A = near-Earth object-relative spacecraft arrival speed, km/s
Δv_D = near-Earth object-relative spacecraft departure speed, km/s
Δv_{TNI} = transnear-Earth object injection change-in-velocity magnitude required to depart a circular Earth parking orbit of radius r_{EPO} and achieve v_{HE}, km/s

Received 26 December 2009; revision received 26 March 2010; accepted for publication 31 March 2010.

*Astrodynamics Consultant, 4203 Moonlight Shadow Court; adamod@earthlink.net. Member AIAA.
†Senior Analyst, Mail Stop 301-150, 4800 Oak Grove Drive; jon.d.giorgini@nasa.gov. Senior Member AIAA.
‡Planetary Scientist, Astromaterials Research and Exploration Science, Mail Code KR; Planetary Science Institute, Tucson, Arizona 85719; paul.a.abell@nasa.gov.
§General Engineer, Intelligent Systems Division, Mail Code TI; NASA Ames Research Center, Moffett Field, California 94035; rob.r.landis@nasa.gov.

δ = near-Earth object geocentric true declination, deg
δ_D = spacecraft Earth departure hyperbolic escape asymptote true declination, deg
δ_R = spacecraft Earth return hyperbolic approach asymptote true declination, deg
μ = sun's reduced mass ($132,712,439,940$ km^3/s^2) [3]
μ_E = Earth's reduced mass ($398,600.440$ km^3/s^2) [3]
ν = near-Earth object heliocentric true anomaly when heliocentric distance is r_M, deg

I. Introduction

DURING mid-2009, the Review of U.S. Human Space Flight Plans Committee (HSFPC) requested a survey of known asteroids be conducted with the objective of identifying near-Earth objects (NEOs) accessible for anticipated human exploration capabilities beyond low-Earth orbit (LEO). This research into NEO accessibility is associated with the HSFPC's flexible path exploration strategy option [1]. The flexible path avoids transporting humans to any near-term exploration destination deep inside an extraterrestrial gravity well, such as the surfaces of the moon or Mars. Instead, human exploration destinations beyond LEO are initially limited to lunar orbit, libration points in the Earth/moon or sun/Earth systems, NEOs, and eventually Mars orbit. After human transport technology and infrastructure have advanced sufficiently beyond LEO, capabilities to land on destinations such as the moon and Mars are anticipated. Pending those milestones, NEOs will be the primary extraterrestrial surfaces with which humans will directly interact on the flexible path. Under NASA's Constellation Program, research into the motivation, techniques, and capabilities supporting NEO exploration had been conducted in 2006 [2], but a methodical survey of accessible NEOs was not within that effort's scope.

The HSFPC-motivated survey of known asteroids identifies accessible NEO destinations through a progressive sequence of stages as follows. These stages are further documented in subsequent sections, together with summaries of their results when applied to a June 2009 survey of the small-body database (SBDB) maintained by the Jet Propulsion Laboratory (JPL). Public access to the SBDB and its associated ephemerides is documented by [3] and is facilitated using JPL's HORIZONS online ephemeris system.[¶]

Stage 1 filters the SBDB based on heliocentric semimajor axis a, eccentricity e, and ecliptic inclination i. Accessibility threshold values for these orbit elements are driven by optimistic launch-vehicle performance assumptions intended to leave no viable NEO destination excluded. Stage 2 uses JPL-maintained ephemerides and searches the time interval from 2020 through 2050 for sufficiently close and predictable encounters between Earth and each NEO identified as potentially accessible by the stage 1 SBDB filter. Beyond-LEO human-mission duration is assumed to be less than a year, due to foreseeable spaceflight technology and residual crew health risks. Each viable human mission to a NEO destination from 2020 through 2050 will therefore fall in the time frame of the corresponding Earth encounter. Stage 3 assumes unperturbed (conic) heliocentric motion and designs optimized round-trip trajectories from Earth, loitering a minimum of 10 days at a NEO destination. Each mission is conducted in a time frame identified by stage 2 for a stage 1 NEO. Accessibility assessments for each NEO mission opportunity are then based on associated trajectory design parameters.

II. Stage 1: Small-Body Database Filter

An initial criterion with which to filter the current SBDB is launch-vehicle Earth escape performance. In obtaining this specification, the strategy is to overestimate ultimately achievable Earth departure propulsive performance such that some exploration destinations accepted by the stage 1 filter as viable will ultimately be found marginally inaccessible by stage 2 and/or stage 3. This stage 1 error condition is preferred to otherwise viable destinations being rejected by overly conservative filtering criteria. The following assumptions are key to launch-vehicle performance estimates.

Assumption A: The mission profile entails a single Ares V launch into a minimal-altitude Earth parking orbit (EPO). Nominal loiter time in this EPO before trans-NEO injection (TNI) and Earth departure stage (EDS) cryogenic propellant depletion is, at most, three orbits.

Assumption B: Post-TNI EDS-injected spacecraft (payload) mass is 45,243 kg. This equates to a minimal capability crew exploration vehicle (CEV) with capacity to impart NEO arrival and NEO departure impulses totaling 3.0 km/s, using storable hypergolic propellant with a specific impulse (I_{SP}) of 314 s. The assumed CEV crew module mass is 9506 kg ([4]: Table 5-1, p. 228), and the CEV wet service module mass is scaled by a factor of 2.62 from its Exploration Systems Architecture Study baseline ([4]: Table 5-2, p. 241) to a value of 35,737 kg (28,165 kg of which is usable propellant mass), thereby achieving the imposed 3.0 km/s capability.

In the context of permissive filtering criteria based on optimistic propulsive performance, it should be noted the filter is not a substitute for detailed mission analysis applied to a specific NEO destination during a specific time frame. In particular, the following disclaimers will apply to destinations deemed accessible by the stage 1 filtration process.

Disclaimer 1: None of the filter criteria deal with mission duration. In general, shorter transit times between the Earth and a NEO destination will require greater propulsive capability from both the launch vehicle and the spacecraft. Consequently, a viable NEO destination according to the filter may prove to be inaccessible when actual trajectory designs are computed for which the transit times comply with human-mission duration limits.

Disclaimer 2: None of the proposed filter criteria deal with launch-vehicle performance losses imposed by EPO equatorial inclination requirements. In general, v_{HE} or EDS-injected payload mass will be reduced if EPO equatorial inclination cannot be designed near 28.5°. Although a NEO destination's i may be small, the mission trajectory's $|\delta_D|$ may be large, because the NEO can attain large $|\delta|$ near Earth. Large $|\delta|$ NEO geometry is likely to arise because, as observed in disclaimer 1, close-Earth approaches are compatible with sufficiently short human-mission transits. The lowest possible EPO inclination supporting a coplanar TNI is equivalent to $|\delta_D|$ ([5], Fig. 6.17).

Because Ares V is far from operational, the relationship between the EDS-injected payload mass and $C3$ or v_{HE} is subject to appreciable revision. The Fig. 1 plot ([6], p. 26) is used to obtain $C3_X = +11.1$ km^2/s^2 (equivalent to $v_{\mathrm{HE}} = 3.33$ km/s) for a minimal 45.2 mT payload mass delivered to TNI from EPO equatorial inclinations near 28.5°. In personal communications with Sumrall [6] during mid-2009, Fig. 1's pedigree had been verified to be highly optimistic in the context of initial human exploration capability beyond LEO. Contrary to the optimistic shaded disclaimer in Fig. 1, Sumrall revealed the associated curve exceeds current Ares V usable payload mass expectations by at least 10%.

The $C3_X$ capability initially defines an annular region in the ecliptic plane for which the reference heliocentric radius r_M is 1 astronomical unit (AU). Circular orbit speed at r_M is v_M:

$$v_M = \sqrt{\frac{\mu}{r_M}} = 29.784692 \text{ km/s}$$

The annulus inner radius r_P is computed, assuming $C3_X$ is applied as a retrograde Earth departure impulse:

$$a_P = \left[\frac{2}{r_M} - \frac{(v_M - \sqrt{C3_X})^2}{\mu}\right]^{-1} = 123,511,664 \text{ km}$$
$$= 0.825624 \text{ AU};$$
$$r_P = 2a_P - r_M = 97,425,458 \text{ km} = 0.651249 \text{ AU}$$

[¶]Data available online at http://ssd.jpl.nasa.gov/?horizons [retrieved 23 March 2010].

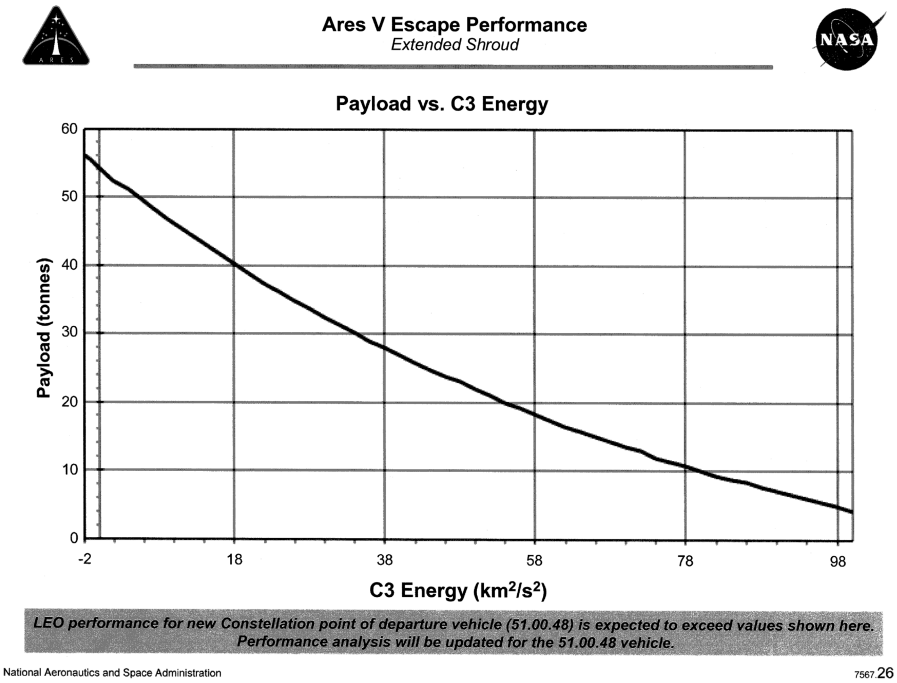

Fig. 1 Ares V EDS-injected payload mass versus Earth departure energy ([6], p. 26).

Similarly, the annulus outer radius r_A is computed, assuming $C3_X$ is applied as a posigrade Earth departure impulse:

$$a_A = \left[\frac{2}{r_M} - \frac{(v_M + \sqrt{C3_X})^2}{\mu}\right]^{-1} = 195,867,433 \text{ km}$$
$$= 1.309293 \text{ AU};$$
$$r_A = 2a_A - r_M = 242,136,996 \text{ km} = 1.618586 \text{ AU}$$

A heliocentric elliptical orbit with apses $r_M \times r_P$ will have eccentricity e_P, and a complementary orbit in the annulus with apses $r_A \times r_M$ will have eccentricity e_A:

$$e_P = \frac{r_M}{a_P} - 1 = 0.211204; \qquad e_A = \frac{r_A}{a_A} - 1 = 0.236229$$

Now, consider a NEO orbit with cataloged heliocentric semimajor axis a and eccentricity e. Effective Earth/NEO heliocentric velocity difference magnitude Δv is to be computed by assuming a close approach between the two orbits, facilitating sufficiently short human-mission transit times. This process begins by determining the NEO orbit's semilatus rectum:

$$p = a(1 - e^2) \tag{1}$$

The polar equation for conic sections then leads to trigonometric expressions for true anomaly ν when the NEO's heliocentric distance is r_M. For purposes of Δv computation, ν is confined to quadrants 1 and 2:

$$\cos\nu = \frac{\frac{p}{r_M} - 1}{e} \tag{2}$$

$$\sin\nu = \sqrt{1 - \cos^2\nu} \tag{3}$$

The component of NEO heliocentric radial velocity at heliocentric distance r_M arises from the time derivative of the polar equation for conic sections:

$$v_R = \sqrt{\frac{\mu}{p}} e \sin\nu \tag{4}$$

The component of NEO heliocentric tangential velocity at heliocentric distance r_M arises from the time derivative of the scalar relationship between ν and angular momentum:

$$v_T = \sqrt{\frac{\mu}{p}}(1 + e\cos\nu) \tag{5}$$

Spacecraft heliocentric speed in the ecliptic plane at Earth departure is determined by the foregoing components:

$$v_E = \sqrt{v_R^2 + v_T^2} \tag{6}$$

assuming Earth's heliocentric orbit is circular with radius r_M, Δv can then be computed:

$$\Delta v = \sqrt{v_R^2 + (v_T - v_M)^2} \tag{7}$$

In cases where $|\cos\nu| > 1$ in Eq. (2), r_M is not intermediate to the NEO orbit's apses. For these instances, e is ignored, Eq. (8) replaces Eqs. (6), and Eq. (9) replaces Eq. (7):

$$v_E = \sqrt{\mu\left(\frac{2}{r_M} - \frac{1}{a}\right)} \tag{8}$$

$$\Delta v = |v_E - v_M| \tag{9}$$

The residual $C3_X - \Delta v^2$ approximates surplus launch energy available to attain the NEO orbit plane. Assuming this residual is positive, the maximum attainable heliocentric inclination i_X can be estimated:

$$i_X = \arctan\left(\frac{\sqrt{C3_X - \Delta v^2}}{v_E}\right) \tag{10}$$

With this formulaic background documented, filter processing and logic are summarized using the following procedural steps.

Step 1: Specific to a NEO destination candidate being filtered, fetch heliocentric semimajor axis a, eccentricity e, and ecliptic inclination i from JPL's SBDB. Proceed to step 2.

Step 2: If $a_P < a < a_A$, proceed to step 3. Otherwise, this NEO is rejected and step 1 may be performed for another candidate.

Step 3: If $a < r_M$ and $e < e_P$ or if $a \geq r_M$ and $e < e_A$, proceed to step 4. Otherwise, this NEO is rejected and step 1 may be performed for another candidate.

Step 4: Compute p from Eq. (1) and $\cos\nu$ from Eq. (2). If $|\cos\nu| > 1$, compute Δv from Eqs. (8) and (9). Otherwise, compute Δv with Eqs. (3–7). Proceed to step 5.

Step 5: If $\Delta v^2 < C3_X$, proceed to step 6. Otherwise, $i_X \equiv 0$, this NEO is rejected, and step 1 may be performed for another candidate.

Step 6: Compute i_X from Eq. (8). If $i < i_X$, this NEO is accepted as a viable destination; otherwise, it is rejected. Step 1 may be performed for another candidate.

Table 1 contains numeric filtering examples applied to current NEO element sets obtained from JPL's HORIZONS ephemeris system. Any value marked with [a] is cause for rejection as a viable destination, while a value marked with [b] signifies a passed criterion necessary for acceptance as a viable NEO destination. Thus, 2000 SG_{344} and 1999 AO_{10} are the only viable destinations in Table 1. Because i_X is a computed filter criterion, Table 1 i_X values are not marked. They are included for comparison with corresponding i values. In Table 1 cases, where $i_X = 0$ per filter step 5, it is then possible to assess i according to filter step 6 and accept or reject its value accordingly. Given that step 5 has already rejected a NEO with $i_X = 0$, assessing i in such cases is purely for reference purposes.

In June 2009, JPL used foregoing computations and logic to filter the current SBDB for viable destinations. The three-dozen NEOs identified by this process are summarized by Table 2 in order of decreasing diameter. Estimated NEO diameters appearing in Table 2 and throughout this paper are based on absolute magnitude and assume a geometric albedo of 0.15. These diameters may therefore be in error by a factor typically ranging from 0.5 to 2. Computation refinements to filter criteria since June 2009, as documented herein, find 1998 HG_{49} Table 2 values produce $i_X = 4.110°$. Although 1998 HG_{49} is rejected in accord with filter step 6, it is retained as a viable human exploration destination throughout this paper because it was reported as such to the HSFPC. Its stage 3 assessment also serves to illustrate mission design characteristics from targeting a marginally inaccessible NEO with respect to stage 1 criteria.

Table 2 Accessible NEO destinations in order of decreasing approximate diameter

Designation	a, AU	e	i, deg	Approx. diameter, m
1996 XB_{27}	1.188926	0.057895	2.465	150
1998 HG_{49}	1.201267	0.113052	4.195	143
2001 BB_{16}	0.854315	0.172498	2.027	104
2003 SM_{84}	1.125731	0.082259	2.795	99
2000 AE_{205}	1.164083	0.137356	4.46	90
2001 QJ_{142}	1.062293	0.086336	3.106	72
1999 AO_{10}	0.911559	0.110971	2.622	57
2008 BT_2	1.173194	0.080773	3.075	47
2008 CX_{118}	1.144725	0.035265	2.42	45
2001 FR_{85}	0.982699	0.027874	5.244	43
2000 SG_{344}	0.977455	0.066908	0.11	38
2007 TF_{15}	1.107648	0.041611	4.185	34
1999 CG_9	1.060676	0.062472	5.158	31
1993 HD	1.126322	0.039145	0.552	30
2005 ER_{95}	1.223111	0.15909	3.336	30
2006 BZ_{147}	1.023436	0.098617	1.409	29
2006 QQ_{56}	0.985266	0.045555	2.797	23
2003 YN_{107}	0.989355	0.013997	4.32	19
2006 UB_{17}	1.140651	0.103764	1.991	19
2007 VU_6	0.976508	0.090496	1.223	17
1999 VX_{25}	0.900003	0.139586	1.663	16
2005 LC	1.133458	0.102199	2.8	15
2001 GP_2	1.037742	0.073962	1.279	14
2005 QP_{87}	1.232859	0.17534	0.268	10
2008 EA_9	1.059154	0.079842	0.424	10
2006 JY_{26}	1.011314	0.083722	1.421	8
2008 HU_4	1.096781	0.078187	1.322	8
2008 KT	1.015719	0.086706	1.991	8
2009 BD	1.008566	0.039071	0.382	8
1991 VG	1.026915	0.049141	1.446	7
2007 UN_{12}	1.053823	0.060455	0.235	6
2008 TS_{10}	1.257401	0.201616	1.459	6
2000 LG_6	0.917411	0.111081	2.833	5
2008 UA_{202}	1.033057	0.068465	0.264	5
2006 RH_{120}	1.033211	0.024507	0.596	4
2008 JL_{24}	1.038238	0.10663	0.55	4

III. Stage 2: Destination Near-Earth Object Encounters with Earth

As noted in Sec. II's SBDB filter disclaimer 1, otherwise viable NEO destinations may never approach Earth closely enough to permit sufficiently short round-trip mission duration $\Delta T < 365$ days. Section IV documents experience with planning practical round trips to NEOs appearing in Table 2. This experience indicates the NEO destination must approach Earth within ~0.1 AU as a necessary condition, leading to sufficiently brief ΔT. Because a NEO's encounter epoch with Earth falls in the time frame of any practical mission, this epoch serves to initiate a more detailed stage 3 mission design.

Stage 2 performs a JPL HORIZONS search for Earth encounters within ~0.1 AU for each Table 2 destination over the time interval from 2020 through 2050. Table 3 summarizes results from these searches, with encounters listed according to decreasing NEO diameter. A subset of Table 2 NEOs has no Earth encounters reportable by HORIZONS. These NEOs are cited in Table 3 with blank cells corresponding to encounter-specific data.

It should be noted that any Table 3 encounter prediction could be affected by unknown systematic biases in the small number ($\ll 150$) of astrometric measurements currently available for any of the referenced NEOs. Prediction uncertainty associated with any NEO destination would be improved by additional astrometric measurements, including data obtained from planetary radar and robotic spacecraft. The fourth column in Table 3 indicates whether or not an encounter search by HORIZONS is aborted before the requested search interval's end on 1 January 2051. An abort is triggered when linearly propagated 3σ uncertainty in NEO position/velocity equates to an encounter epoch uncertainty exceeding ± 10 days. Consequently, a "Yes" in this column indicates reported encounters may be inaccurate (particularly in later years), and other encounters leading to possible mission opportunities from 2020 through 2050 may be missing altogether. A "No" indicates higher confidence in finding and reporting all Earth encounters pertaining to a specific NEO from 2020 through 2050. Even if encounter date uncertainty is less than ± 10 days, position uncertainty may extend over millions of kilometers.

Table 1 SBDB filtration examples

Filter quantity	2000 SG_{344}	1999 AO_{10}	2003 YS_{70}	(433) Eros	(99,942) Apophis	(25,143) Itokawa	(4660) Nereus
a, AU	0.982804[b]	0.910773[b]	1.317601[a]	1.458252[a]	0.922378[a]	1.322775[a]	1.488671[a]
e	0.065447[b]	0.112650[b]	0.252754[a]	0.222907[b]	0.191055[a]	0.279444[a]	0.360147[a]
i, deg	0.108[b]	2.263[b]	0.403[a]	10.829[a]	3.331[a]	1.728[a]	1.433[a]
Δv, km/s	1.889514[b]	2.207358[b]	4.196370[a]	4.360665[a]	5.194682[a]	5.604860[a]	6.778057[a]
i_X, deg	5.310	5.041	0	0	0	0	0

[a]Rejected as a viable destination.
[b]Passed criterion necessary for acceptance as a viable NEO destination.

Table 3 Earth encounters with accessible NEO destinations

Encounter no.	Designation	Approx. diameter, m	Abort before 2051	Encounter date	r_{MIN}, AU	v_{MIN}, km/s
1	1996 XB_{27}	150	No	29 July 2027	0.156919	1.696
2	1996 XB_{27}	150	No	19 May 2049	0.115122	0.852
3	1998 HG_{49}	143	No	27 July 2031	0.163567	1.055
4	2001 BB_{16}	104	No	8 March 2020	0.091314	6.489
5	2001 BB_{16}	104	No	6 Jan. 2035	0.037748	4.860
6	2001 BB_{16}	104	No	7 March 2039	0.041600	4.698
7	2003 SM_{84}	99	No	26 July 2040	0.063785	2.589
8	2003 SM_{84}	99	No	20 July 2046	0.051413	1.503
9	2000 AE_{205}	90	No	28 Nov. 2048	0.068063	2.848
10	2001 QJ_{142}	72	Yes	9 May 2024	0.059030	2.239
11	1999 AO_{10}	57	No	11 Feb. 2026	0.026794	2.679
12	1999 AO_{10}	57	No	26 Dec. 2045	0.076668	5.095
13	2008 BT_{2}	47	Yes	16 March 2022	0.086192	1.547
14	2008 CX_{118}	45	Yes	18 July 2024	0.090004	1.301
15	2001 FR_{85}	43	No	21 March 2039	0.045029	3.162
16	2001 FR_{85}	43	No	28 Sept. 2039	0.030896	2.860
17	2001 FR_{85}	43	No	28 March 2040	0.058253	3.179
18	2001 FR_{85}	43	No	14 Aug. 2040	0.096517	3.486
19	2000 SG_{344}	38	Yes	7 May 2028	0.019622	2.034
20	2000 SG_{344}	38	Yes	16 Feb. 2029	0.052714	1.471
21	2000 SG_{344}	38	Yes	28 July 2029	0.034215	1.189
22	2000 SG_{344}	38	Yes	21 Nov. 2029	0.045229	1.253
	2007 TF_{15}	34	No	——	——	——
23	1999 CG_{9}	31	Yes	6 Feb. 2034	0.045397	2.738
	1993 HD	30	Yes	——	——	——
24	2005 ER_{95}	30	Yes	23 March 2028	0.033469	2.636
25	2006 BZ_{147}	29	No	25 Feb. 2035	0.019218	3.897
26	2006 BZ_{147}	29	No	9 May 2036	0.094208	3.083
27	2006 BZ_{147}	29	No	6 Aug. 2037	0.052206	2.041
28	2006 BZ_{147}	29	No	26 Aug. 2038	0.098697	6.195
29	2006 QQ_{56}	23	No	22 April 2050	0.047459	1.579
30	2006 QQ_{56}	23	No	7 Aug. 2050	0.033290	1.666
	2003 YN_{107}	19	No	——	——	——
31	2006 UB_{17}	19	Yes	3 Oct. 2034	0.077556	3.772
32	2007 VU_{6}	17	Yes	6 Oct. 2034	0.032501	2.324
33	1999 VX_{25}	16	Yes	15 Sept. 2028	0.048372	4.497
34	1999 VX_{25}	16	Yes	28 Sept. 2034	0.026033	2.938
35	2005 LC	15	Yes	30 May 2040	0.030686	2.740
36	2001 GP_{2}	14	Yes	3 Oct. 2020	0.008029	2.486
37	2001 GP_{2}	14	Yes	19 April 2048	0.089772	5.176
38	2005 QP_{87}	10	No	18 Sept. 2031	0.032880	3.533
39	2008 EA_{9}	10	Yes	25 April 2020	0.074595	1.321
40	2008 EA_{9}	10	Yes	15 Nov. 2033	0.078024	3.695
	2006 JY_{26}	8	No	——	——	——
41	2008 HU_{4}	8	Yes	22 Jan. 2047	0.090688	1.437
	2008 KT	8	No	——	——	——
42	2009 BD	8	Yes	27 March 2034	0.092508	3.703
43	2009 BD	8	Yes	1 Sept. 2034	0.093932	1.598
44	1991 VG	7	No	7 Nov. 2038	0.073178	3.052
45	1991 VG	7	No	29 May 2039	0.060540	1.483
46	2007 UN_{12}	6	Yes	4 July 2020	0.043224	2.897
47	2007 UN_{12}	6	Yes	8 Jan. 2021	0.095489	2.013
48	2007 UN_{12}	6	Yes	30 April 2049	0.089922	1.770
49	2008 TS_{10}	6	Yes	31 July 2032	0.092398	6.061
50	2000 LG_{6}	5	No	24 June 2036	0.026258	2.429
51	2008 UA_{202}	5	Yes	18 May 2028	0.088711	4.943
52	2008 UA_{202}	5	Yes	20 Oct. 2029	0.013617	2.807
53	2006 RH_{120}	4	Yes	8 Aug. 2028	0.028815	0.215
54	2006 RH_{120}	4	Yes	7 June 2044	0.064970	1.180
55	2008 JL_{24}	4	No	5 March 2026	0.060990	2.403
56	2008 JL_{24}	4	No	21 June 2026	0.093079	1.991
57	2008 JL_{24}	4	No	9 Dec. 2043	0.018955	3.319
58	2008 JL_{24}	4	No	17 May 2045	0.016299	3.269

IV. Stage 3: Destination Near-Earth Object Human-Mission Trajectory Design

In the context of human NEO exploration, viability of a Table 3 encounter must ultimately be assessed with a trajectory design in the corresponding time frame. Such a design consists of an outbound leg departing Earth and arriving at the NEO destination 10 days or more before the return leg departs the NEO bound for Earth. Heliocentric conic arcs approximate both trajectory legs to sufficient accuracy. Therefore, Earth and NEO heliocentric positions at the termini of each trajectory leg are among the Lambert boundary conditions (LBCs) leading to trajectory solutions supporting mission viability assessment. Heliocentric NEO positions associated with these Lambert solutions are imported from JPL's HORIZONS ephemeris system, while those for Earth are computed via general perturbations theory [7] as a convenience, minimizing data import labor. Heliocentric Earth position deviations between [3,7] ephemerides

are less than 300 km and are of negligible consequence in this context, because associated Lambert solutions completely ignore Earth gravity. To ensure reasonably brief transit times for each mission leg compatible with human endurance, LBCs are constrained such that only short way (type I) trajectory solutions spanning less than a 180° heliocentric transfer angle are produced.

Pork-chop charts (PCCs) are the primary aid in selecting optimal departure and arrival dates for outbound and return trajectory legs. A PCC is an array of values, with each element corresponding to a unique Lambert heliocentric trajectory solution. Each column in a PCC array is dedicated to a departure date, and each row is dedicated to an arrival date. On the outbound trajectory leg, PCC arrays composed of v_{HE}, δ_D, or Δv_A values may be relevant. For the return trajectory leg, PCC arrays composed of Δv_D, v_{EI}, or δ_R values may be relevant. Values appearing in a PCC are conditionally formatted to visually aid optimization. When populated by speed values, PCC elements greater than 5 km/s are shaded light gray, and those less than 2.5 km/s are shaded bold. When populated by declination values, PCC elements whose magnitudes exceed 57° are shaded light gray, and those for which the magnitudes are less than 28.5° are shaded bold. Intermediate PCC values are italicized. Optimization criteria are as follows in order of decreasing priority.

Priority 1: Minimize Δv_A and Δv_D at the expense of v_{HE} as necessary. Following launch into an EPO of unknown geocentric radius r_{EPO}, three propulsive impulses are assumed for the mission. The TNI impulse Δv_{TNI} occurs in the EPO, using relatively efficient cryogenic propellant. If r_{EPO} is known, Δv_{TNI} can be computed from a PCC's v_{HE} value as follows:

$$\Delta v_{\mathrm{TNI}} = \sqrt{v_{\mathrm{HE}}^2 + \frac{2\mu_E}{r_{\mathrm{EPO}}}} - \sqrt{\frac{\mu_E}{r_{\mathrm{EPO}}}}$$

The final two impulses occur at NEO arrival and departure (Earth-return braking is assumed to be through atmospheric friction) using relatively inefficient but storable hypergolic propellant. Because of this inefficiency, Δv_A and Δv_D pose a greater obstacle to NEO accessibility than does v_{HE}. Effectively zero priority is given to minimizing v_{EI}, because it has no propulsive cost. Heat shield thermal loads are relatable to v_{EI}, but Earth atmospheric-entry shielding limits of future spacecraft are currently uncertain. Note the fastest v_{EI} experienced by humans was logged during Apollo 10 at 11.069 km/s ([8], p. 581).

Priority 2: Minimize any $|\delta_D| > 28.5°$ to the extent permitted by v_{HE}, Δv_A, and Δv_D. As observed in Sec. II's SBDB filter disclaimer 2, a geocentric Earth departure trajectory's asymptotic declination magnitude $|\delta_D|$ sets a lower limit on EPO equatorial inclination. Assuming a Florida launch into a posigrade EPO, $|\delta_D| > 28.5°$ will impose a performance loss in achieving EPO. At $|\delta_D| > 57°$, additional launch performance losses are likely to be imposed by range safety constraints. Any of these losses will reduce the EDS propellant available to perform TNI for a given spacecraft payload mass at a given r_{EPO}. Effectively, zero priority is given to minimizing $|\delta_R|$, because it imposes no propulsive cost.

Priority 3: Maintain round-trip mission duration ΔT at less than a year. This constraint addresses crew microgravity and radiation exposure concerns, but it may require considerable modification as

◇	A	B	C	D	E	F	G	H	I	J	K	L
1	**1999 AO10**					**Earth Depart Date**						
2	**Arrive Date**	7/31/25	8/10/25	8/20/25	8/30/25	9/9/25	9/19/25	9/29/25	10/9/25	10/19/25	10/29/25	11/8/25
3	**9/19/25**	10.868	12.973	16.807	24.824	49.488						
4	**9/29/25**	7.620	8.639	10.389	13.511	20.101	40.337					
5	**10/9/25**	5.374	5.863	6.710	8.107	10.664	16.076	32.438				
6	**10/19/25**	***3.789***	***4.007***	***4.427***	5.097	6.264	8.425	12.840	26.154			
7	**10/29/25**	***2.690***	***2.767***	***2.978***	***3.320***	***3.921***	***4.984***	6.814	10.563	21.658		
8	**11/8/25**	**1.984**	**1.987**	**2.097**	**2.288**	***2.646***	***3.263***	***4.223***	5.896	9.189	18.799	
9	**11/18/25**	**1.613**	**1.575**	**1.631**	**1.751**	**1.998**	**2.406**	***2.995***	***3.939***	5.477	8.450	17.220
10	**11/28/25**	**1.496**	**1.424**	**1.443**	**1.520**	**1.703**	**1.990**	**2.384**	***2.988***	***3.863***	5.275	8.069
11	**12/8/25**	**1.522**	**1.408**	**1.389**	**1.430**	**1.565**	**1.766**	**2.038**	**2.448**	***2.992***	***3.788***	5.119
12	**12/18/25**	**1.606**	**1.429**	**1.368**	**1.373**	**1.466**	**1.603**	**1.788**	**2.072**	**2.421**	***2.902***	***3.643***
13	**12/28/25**	**1.713**	**1.434**	**1.324**	**1.295**	**1.352**	**1.440**	**1.561**	**1.757**	**1.979**	**2.275**	***2.714***
14	**1/7/26**	**1.863**	**1.398**	**1.232**	**1.173**	**1.204**	**1.254**	**1.328**	**1.461**	**1.596**	**1.773**	**2.037**
15	**1/17/26**	**2.260**	**1.290**	**1.066**	**0.994**	**1.013**	**1.040**	**1.081**	**1.170**	**1.244**	**1.343**	**1.497**
16	**1/27/26**	57.640	**0.988**	**0.791**	**0.757**	**0.788**	**0.806**	**0.826**	**0.885**	**0.916**	**0.962**	**1.047**
17	**2/6/26**	58.843	46.301	**0.854**	**0.651**	**0.632**	**0.619**	**0.611**	**0.639**	**0.636**	**0.644**	**0.684**
18	**2/16/26**	58.696	58.870	26.659	**1.851**	**1.020**	**0.752**	**0.622**	**0.567**	**0.516**	**0.490**	**0.493**
19	**2/26/26**	58.433	58.720	58.892	23.470	***2.832***	**1.516**	**1.058**	**0.838**	**0.710**	**0.643**	**0.612**
20	**3/8/26**	58.052	58.444	58.769	58.845	22.678	***3.705***	**2.025**	**1.432**	**1.151**	**1.008**	**0.932**
21	**3/18/26**	57.550	58.044	58.482	58.781	58.754	22.910	***4.483***	***2.514***	**1.825**	**1.510**	**1.345**
22	**3/28/26**	56.921	57.517	58.062	58.488	58.772	58.689	23.986	5.195	***2.982***	**2.215**	**1.859**
23	**4/7/26**	56.162	56.858	57.508	58.048	58.471	58.792	58.616	26.192	5.878	***3.416***	***2.569***

Fig. 2 Geocentric Earth departure to 1999 AO_{10} hyperbolic excess speed v_{HE} PCC values in km/s.

◇	A	B	C	D	E	F	G	H	I	J	K	L
1	**1999 AO10**					**Earth Depart Date**						
2	**Arrive Date**	7/31/25	8/10/25	8/20/25	8/30/25	9/9/25	9/19/25	9/29/25	10/9/25	10/19/25	10/29/25	11/8/25
3	9/19/25	**-12.431**	**-12.203**	**-11.817**	**-11.391**	**-11.041**						
4	9/29/25	**-11.075**	**-10.952**	**-10.649**	**-10.237**	**-9.800**	**-9.547**					
5	10/9/25	**-7.895**	**-7.861**	**-7.672**	**-7.334**	**-6.914**	**-6.690**	**-6.574**				
6	10/19/25	**-2.210**	**-2.253**	**-2.229**	**-2.030**	**-1.750**	**-1.787**	**-1.875**	**-2.033**			
7	10/29/25	**7.019**	**6.895**	**6.609**	**6.514**	**6.402**	**5.687**	**5.005**	**4.263**	**3.613**		
8	11/8/25	**20.762**	**20.539**	**19.592**	**18.804**	**17.722**	**15.613**	**13.780**	**11.928**	**10.298**	**9.345**	
9	11/18/25	*38.095*	*37.665*	*35.439*	*33.255*	*30.324*	**26.154**	**22.777**	**19.508**	**16.702**	**14.875**	**13.676**
10	11/28/25	*54.706*	*53.635*	*49.493*	*45.379*	*40.251*	*34.246*	*29.619*	**25.212**	**21.495**	**18.973**	**17.035**
11	12/8/25	66.503	64.042	57.794	*51.992*	*45.346*	*38.461*	*33.284*	**28.327**	**24.161**	**21.272**	**18.848**
12	12/18/25	73.094	68.756	60.829	*53.999*	*46.675*	*39.605*	*34.361*	*29.272*	**24.984**	**21.989**	**19.304**
13	12/28/25	76.358	70.255	61.030	*53.509*	*45.867*	*38.827*	*33.700*	*28.663*	**24.405**	**21.461**	**18.666**
14	1/7/26	78.154	70.607	59.776	*51.452*	*43.520*	*36.529*	*31.603*	**26.722**	**22.577**	**19.803**	**17.013**
15	1/17/26	78.148	70.277	*56.384*	*46.895*	*38.778*	*31.997*	**27.489**	**22.983**	**19.084**	**16.658**	**14.024**
16	1/27/26	**-2.880**	64.335	*43.388*	*34.004*	**27.549**	**22.165**	**18.950**	**15.573**	**12.295**	**10.614**	**8.474**
17	2/6/26	**-15.383**	*-52.871*	**-27.744**	**-11.113**	**-3.617**	**-2.256**	**-1.209**	**-1.012**	**-2.714**	**-2.706**	**-3.407**
18	2/16/26	**-16.466**	**-19.489**	-75.385	-57.699	*-47.673*	*-42.234*	*-37.595*	*-33.047*	*-33.077*	*-30.383*	**-28.074**
19	2/26/26	**-17.314**	**-19.827**	**-23.252**	-80.766	-65.619	-62.523	-59.512	*-56.077*	*-54.865*	*-49.481*	*-44.826*
20	3/8/26	**-18.084**	**-20.336**	**-22.704**	**-26.509**	-85.203	-69.399	-65.601	-61.513	-57.536	*-50.529*	*-44.591*
21	3/18/26	**-18.807**	**-20.864**	**-22.822**	**-24.961**	*-29.031*	-89.412	-69.672	-63.942	-58.121	*-50.326*	*-43.532*
22	3/28/26	**-19.491**	**-21.377**	**-23.069**	**-24.649**	**-26.450**	*-30.578*	-85.401	-68.197	-60.574	*-51.959*	*-44.221*
23	4/7/26	**-20.137**	**-21.862**	**-23.338**	**-24.584**	**-25.694**	**-27.056**	*-30.920*	-80.194	-65.833	*-55.827*	*-46.831*

Fig. 3 Geocentric Earth departure to 1999 AO_{10} asymptotic declination δ_D PCC values in degrees.

	A	B	C	D	E	F	G	H	I	J	K	L
1	1999 AO10					Earth Depart Date						
2	Arrive Date	7/31/25	8/10/25	8/20/25	8/30/25	9/9/25	9/19/25	9/29/25	10/9/25	10/19/25	10/29/25	11/8/25
3	9/19/25	20.273	22.827	26.927	35.043	59.549						
4	9/29/25	16.192	17.633	19.662	22.941	29.476	49.390					
5	10/9/25	13.042	13.894	14.988	16.546	19.092	24.258	40.191				
6	10/19/25	10.529	11.038	11.649	12.446	13.600	15.544	19.589	32.310			
7	10/29/25	8.496	8.791	9.129	9.545	10.100	10.946	12.436	15.653	26.076		
8	11/8/25	6.841	6.999	7.176	7.386	7.654	8.044	8.684	9.886	12.614	21.617	
9	11/18/25	5.494	5.564	5.644	5.741	5.866	6.051	6.355	6.902	7.997	10.520	18.826
10	11/28/25	*4.401*	*4.416*	*4.442*	*4.481*	*4.538*	*4.633*	*4.800*	5.099	5.664	6.779	9.282
11	12/8/25	*3.523*	*3.507*	*3.509*	*3.526*	*3.561*	*3.626*	*3.743*	*3.947*	*4.308*	*4.944*	6.126
12	12/18/25	*2.832*	*2.804*	*2.806*	*2.828*	*2.868*	*2.935*	*3.044*	*3.217*	*3.490*	*3.920*	*4.615*
13	12/28/25	**2.317**	**2.288**	**2.312**	**2.357**	**2.419**	*2.504*	*2.620*	*2.781*	*3.008*	*3.325*	*3.785*
14	1/7/26	**1.983**	**1.951**	**2.017**	**2.097**	**2.184**	**2.285**	**2.406**	*2.554*	*2.743*	*2.984*	*3.302*
15	1/17/26	**1.922**	**1.794**	**1.919**	**2.029**	**2.130**	**2.233**	**2.344**	**2.470**	*2.620*	*2.796*	*3.014*
16	1/27/26	56.161	**1.852**	**2.042**	**2.145**	**2.228**	**2.308**	**2.392**	**2.484**	*2.588*	*2.706*	*2.844*
17	2/6/26	57.459	45.980	*2.685*	*2.507*	**2.481**	**2.495**	*2.525*	*2.567*	*2.620*	*2.680*	*2.749*
18	2/16/26	57.315	57.468	27.159	*3.650*	*2.998*	*2.814*	*2.739*	*2.707*	*2.696*	*2.694*	*2.699*
19	2/26/26	57.206	57.481	57.616	24.097	*4.510*	*3.430*	*3.084*	*2.916*	*2.815*	*2.740*	*2.678*
20	3/8/26	57.117	57.513	57.798	57.882	23.369	5.233	*3.777*	*3.277*	*3.015*	*2.838*	*2.698*
21	3/18/26	57.037	57.556	57.969	58.259	58.265	23.643	5.830	*4.037*	*3.387*	*3.028*	*2.778*
22	3/28/26	56.956	57.598	58.137	58.566	58.860	58.778	24.790	6.334	*4.209*	*3.411*	*2.959*
23	4/7/26	56.860	57.626	58.293	58.853	59.298	59.598	59.448	27.130	6.779	*4.298*	*3.354*

Fig. 4 1999 AO_{10}-relative arrival speed Δv_A PCC values in km/s.

	A	B	C	D	E	F	G	H	I	J	K	L
1	Earth Return					1999 AO10 Depart Date						
2	Date	11/28/25	12/8/25	12/18/25	12/28/25	1/7/26	1/17/26	1/27/26	2/6/26	2/16/26	2/26/26	3/8/26
3	12/3/25	31.575										
4	12/13/25	9.908	29.526									
5	12/23/25	5.500	9.016	26.785								
6	1/2/26	*3.533*	*4.808*	7.849	23.295							
7	1/12/26	**2.366**	*2.920*	*3.957*	6.458	19.189						
8	1/22/26	**1.559**	**1.805**	**2.223**	*3.023*	*4.962*	14.811					
9	2/1/26	**0.972**	**1.077**	**1.256**	**1.573**	**2.185**	*3.653*	11.015				
10	2/11/26	**0.592**	**0.647**	**0.750**	**0.928**	**1.229**	**1.781**	*3.051*	9.281			
11	2/21/26	**0.555**	**0.615**	**0.718**	**0.875**	**1.109**	**1.475**	**2.117**	*3.577*	10.768		
12	3/3/26	**0.808**	**0.865**	**0.962**	**1.105**	**1.308**	**1.602**	**2.061**	*2.872*	*4.746*	14.147	
13	3/13/26	**1.142**	**1.178**	**1.257**	**1.377**	**1.548**	**1.788**	**2.139**	*2.691*	*3.680*	6.018	17.875
14	3/23/26	**1.497**	**1.496**	**1.543**	**1.633**	**1.767**	**1.956**	**2.225**	*2.621*	*3.249*	*4.409*	7.194
15	4/2/26	**1.870**	**1.810**	**1.813**	**1.862**	**1.954**	**2.093**	**2.291**	*2.575*	*2.998*	*3.696*	5.016
16	4/12/26	**2.285**	**2.131**	**2.072**	**2.073**	**2.118**	**2.205**	**2.340**	*2.537*	*2.826*	*3.279*	*4.056*
17	4/22/26	*2.788*	**2.479**	**2.332**	**2.271**	**2.263**	**2.298**	**2.375**	*2.501*	*2.692*	*2.997*	*3.506*
18	5/2/26	*3.500*	*2.894*	*2.609*	**2.464**	**2.394**	**2.374**	**2.396**	**2.462**	*2.579*	*2.785*	*3.143*
19	5/12/26	*4.798*	*3.471*	*2.936*	*2.670*	*2.523*	**2.443**	**2.411**	**2.423**	**2.482**	*2.620*	*2.889*
20	5/22/26	8.636	*4.500*	*3.388*	*2.911*	*2.657*	*2.508*	**2.421**	**2.383**	**2.395**	**2.485**	*2.701*
21	6/1/26	48.638	7.391	*4.185*	*3.243*	*2.815*	*2.574*	**2.426**	**2.341**	**2.314**	**2.371**	*2.558*
22	6/11/26	61.227	39.182	6.378	*3.832*	*3.036*	*2.654*	**2.432**	**2.299**	**2.239**	**2.274**	**2.448**
23	6/21/26	61.186	60.270	31.151	5.460	*3.434*	*2.770*	**2.442**	**2.255**	**2.165**	**2.187**	**2.360**

Fig. 5 1999 AO_{10}-relative departure speed Δv_D PCC values in km/s.

the means to mitigate these concerns are developed. Although a low-priority constraint in this list, sufficiently short ΔT is actually enforced by stage 1's SBDB filter and by previously noted LBCs confining trajectory solutions to less than a 180° heliocentric transfer angle. Thus, missions with small v_{HE}, Δv_A, and Δv_D values naturally tend to possess sufficiently short ΔT values.

As an illustration of optimized NEO human-mission trajectory designs, using data from Sec. III, consider Table 3's Earth encounter no. 11 with 1999 AO_{10}. Figures 2–5 are PCCs presenting v_{HE}, δ_D, Δv_A, and Δv_D values key to trajectory design in the encounter no. 11 time frame. Data circumscribed by boxes in these PCCs correspond to optimal departure and arrival dates.

In arriving at optimal dates from the ensuing PCC data, two conflicting trends must be resolved. The primary conflict arises between Δv_A and Δv_D values in Figs. 4 and 5, where minimal Δv_D in Fig. 5 is obtained for 1999 AO_{10} departure dates well before Fig. 4's minimum Δv_A for 1999 AO_{10} arrival dates. Fortunately, a reasonable compromise between Δv_A and Δv_D trends can be achieved by selecting 1999 AO_{10} arrival on 7 January 2026, with departure 10 days later. At the expense of greater mission duration ΔT, further Δv_A reduction could be achieved by selecting an earlier Earth departure date. Unfortunately, launch dates much earlier than 19 September 2025 lead to a second conflicting trend in Fig. 3. Shifting the Earth departure date earlier, while maintaining the 1999 AO_{10} arrival on 7 January 2026 in Fig. 3 rapidly increases δ_D, incurring significant launch-performance losses and likely range safety constraint violations by late August 2026. Choice of outbound leg departure and arrival dates is fortunately supported by a reasonably small v_{HE} value in Fig. 2.

To summarize, PCC data in Fig. 2–5 facilitate an optimized human-mission trajectory design, with major events listed in Table 4.

Outbound and return legs of the optimized 1999 AO_{10} trajectory are plotted geocentrically in Fig. 6.

Stage 3 mission assessments akin to the foregoing 1999 AO_{10} example have been performed for some additional Table 3 Earth encounters with accessible NEO destinations. Results from these trajectory designs are summarized in Table 5.

The sum $\Delta v_A + \Delta v_D$ for each of the 20 Table 5 missions is plotted against the associated NEO/Earth encounter's r_{MIN} from Table 3 in Fig. 7. A correlation between these two variables is evident, such that all Fig. 7 points fall above the dotted line $\Delta v_A + \Delta v_D$ km/s $= 25 r_{MIN}$ AU. The 25 km/s/AU slope in this relationship is reasonably in accord with constant speed transits, covering r_{MIN} in six months. For example, consider $r_{MIN}=$ 0.04 AU $= 5,983,915$ km. Covering this distance in six months (182 days or 15,724,800 s) requires a constant speed of 0.381 km/s,

Table 4 Major events in an optimized human mission to NEO 1999 AO_{10}

Date	Event
19 Sept. 2025	Depart Earth: $v_{HE} = 1.254$ km/s, $\delta_D = +36.529°$
7 Jan. 2026	Arrive 1999 AO_{10}: $\Delta v_A = 2.285$ km/s
17 Jan. 2026	Depart 1999 AO_{10}: $\Delta v_D = 1.475$ km/s
21 Feb. 2026	Arrive Earth: $v_{EI} = 11.332$ km/s, $\delta_R = -9.570°$, $\Delta T = 155$ days

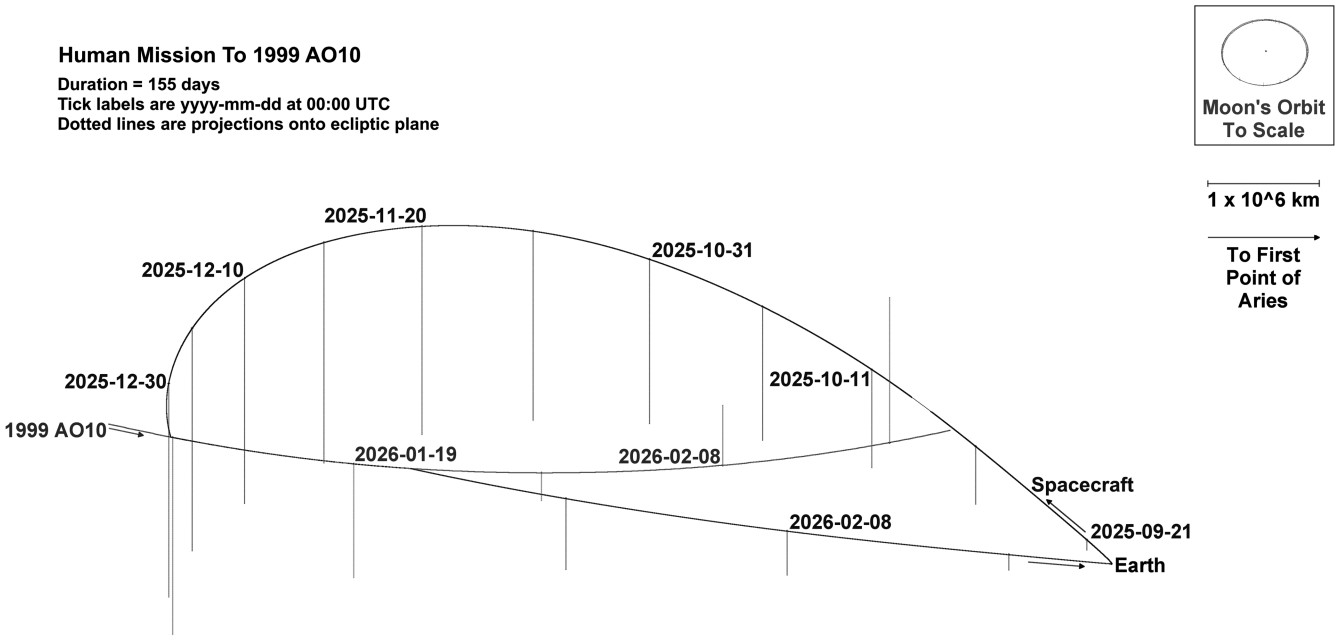

Fig. 6 Geocentric 1999 AO_{10} human-mission trajectory.

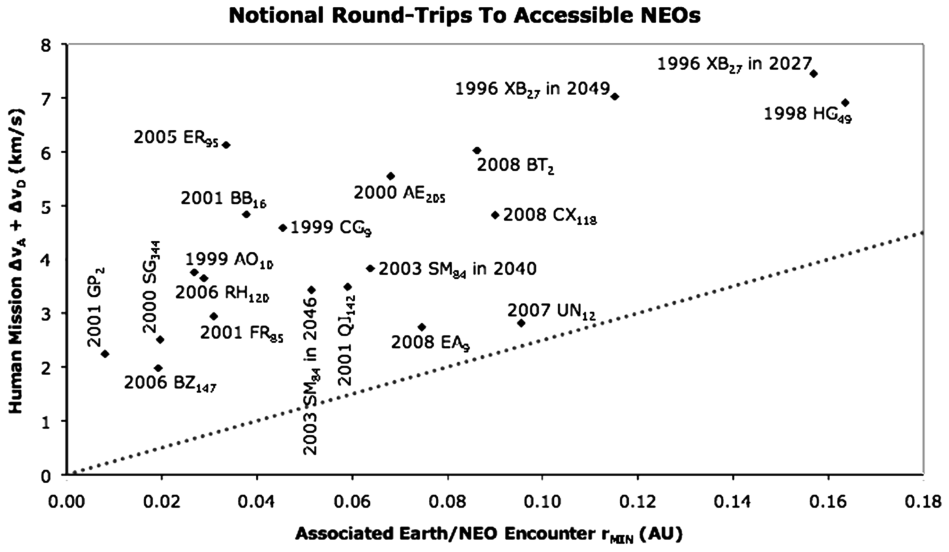

Fig. 7 Correlation between $\Delta v_A + \Delta v_D$ and NEO/Earth encounter r_{MIN} in Table 5 missions.

approximating Δv_A or Δv_D in this simplified model. When doubled to approximate $\Delta v_A + \Delta v_D$, in Fig. 7, constant speed change at the NEO is 0.762 km/s. The constant speed equivalent slope from this example is then $0.762/0.04 = 19.0$ km/s/AU. The dotted line passing through the Fig. 7 origin with the 25 km/s/AU slope should therefore pass below all real-world mission design points, excepting those of nearly 1-year duration for which the NEO destinations have nearly zero geocentric relative motion at spacecraft arrival and departure.

With the stage 1 filter's assumption B equating to $\Delta v_A + \Delta v_D < 3$ km/s, Fig. 7's correlation would impose a stage 2 encounter search constraint of $r_{MIN} < 3/25 = 0.12$ AU. This criterion is in close agreement with the encounter search strategy documented in Sec. III. At a more optimistic capability equivalent to $\Delta v_A + \Delta v_D < 5$ km/s, stage 2 searches constrained to $r_{MIN} < 5/25 = 0.2$ AU would be appropriate. Because stage 2 encounter searches with $r_{MIN} > 0.1$ AU were only performed for 1996 XB_{27} and 1998 HG_{49}, the two largest accessible NEOs, other Fig. 7 points for missions to smaller destinations undoubtedly exist for $r_{MIN} > 0.1$ AU. It remains to be verified where these points fall with respect to the $\Delta v_A + \Delta v_D$ km/s $= 25 r_{MIN}$ AU line. Finally, note how the lone mission opportunity to marginally inaccessible 1998 HG_{49} becomes an outlying point in Fig. 7. Although this mission's $\Delta v_A + \Delta v_D$ is competitive with those pertaining to the two 1996 XB_{27} missions, its v_{EI} is more than 0.4 km/s greater than that of either 1996 XB_{27} mission and is the largest such value in Table 5.

V. Conclusions

A three-stage survey process to identify and assess human NEO mission prospects has been documented and applied to the JPL's current SBDB in the context of anticipated human exploration

Table 5 Summary of optimized mission designs associated with some Table 3 encounters

Encounter no.	Designation	∼Diam, m	Launch date	v_{HE}, km/s	Δv_A, km/s	Δv_D, km/s	v_{EI}, km/s	ΔT, days
1	1996 XB_{27}	150	31 Jan. 2027	4.327	3.937	3.514	11.230	260
2	1996 XB_{27}	150	1 Jan. 2049	2.586	3.693	3.331	11.431	290
3	1998 HG_{49}	143	21 April 2031	2.504	3.712	3.200	11.847	240
5	2001 BB_{16}	104	30 Nov. 2034	2.425	1.964	2.871	11.227	240
7	2003 SM_{84}	99	20 Feb. 2040	1.383	2.780	1.051	11.236	210
8	2003 SM_{84}	99	22 March 2046	1.467	2.054	1.378	11.177	180
9	2000 AE_{205}	90	11 June 2048	2.868	2.796	2.750	11.262	220
10	2001 QJ_{142}	72	10 April 2024	2.115	1.102	2.386	11.352	200
11	1999 AO_{10}	57	19 Sept. 2025	1.254	2.285	1.475	11.332	155
13	2008 BT_2	47	12 Dec. 2021	1.569	2.921	3.104	11.425	270
14	2008 CX_{118}	45	11 Jan. 2024	2.164	2.551	2.273	11.162	350
16	2001 FR_{85}	43	30 Aug. 2039	1.642	2.094	0.847	11.513	210
19	2000 SG_{344}	38	9 Feb. 2028	0.298	0.754	1.754	11.124	310
23	1999 CG_9	31	30 Dec. 2033	1.867	2.290	2.296	11.355	220
24	2005 ER_{95}	30	11 Dec. 2027	0.749	3.459	2.666	11.107	260
25	2006 BZ_{147}	29	29 Jan. 2035	2.553	0.919	1.060	11.572	360
36	2001 GP_2	14	9 Dec. 2019	1.522	2.073	0.170	11.339	304
39	2008 EA_9	10	30 Nov. 2019	2.186	0.979	1.762	11.214	155
47	2007 UN_{12}	6	18 July 2020	2.679	1.109	1.707	11.346	190
53	2006 RH_{120}	4	31 March 2028	0.901	2.042	1.606	11.224	130

capabilities beyond LEO. No less than 36 potentially accessible human-mission destinations were culled from the SBDB in June 2009. Over the interval from 2020 to 2050, these destinations give rise to at least 58 potential mission opportunities coinciding with NEO encounters closer than ∼0.1 AU from Earth. Of these opportunities, half a dozen require storable propulsive capability at the NEO destination, less than the 3 km/s change-in-velocity assumed as an initial accessibility criterion. If this capability is augmented, viable mission opportunities proliferate dramatically. As the SBDB is populated with an order of magnitude more NEOs in the coming decades, opportunities using any exploration capability appreciably beyond that achieved during the Apollo program will increase by at least a factor of 10. To illustrate this population explosion, stage 1's filter again polled the SBDB in November 2009. From discoveries catalogued in the five months since June 2009, 2009 OS_5 and 2009 RT_1 have joined the 36 initially identified accessible NEOs as potential human exploration destinations.

Acknowledgments

The authors wish to acknowledge two significant technical contributors to the small-body database survey of accessible human exploration destinations. At the NASA Marshall Space Flight Center, J. Phil Sumrall supplemented Fig. 1 with detailed pedigree information on Ares V performance data that were communicated in a timely fashion. At the Jet Propulsion Laboratory, Ted H. Sweetser reviewed the stage 1 filter in detail, helping identify and correct a critical error.

References

[1] Review of U.S. Human Spaceflight Plans Committee, "Seeking a Human Spaceflight Program Worthy of a Great Nation," NASA, Oct. 2009.

[2] Landis, R. R., Abell, P. A., Korsmeyer, D. J., Jones, T. D., and Adamo, D. R., "Piloted Operations at a Near-Earth Object (NEO)," *Acta Astronautica*, Vol. 65, Elsevier, Amsterdam, 2009, pp. 1689–1697.

[3] Giorgini, J. D., Yeomans, D. K., Chamberlin, A. B., Chodas, P. W., Jacobson, R. A., Keesey, M. S., Lieske, J. H., Ostro, S. J., Standish, E. M., and Wimberly, R. N., "JPL's On-Line Solar System Data Service," *Bulletin of the American Astronomical Society*, Vol. 28, No. 3, 1996, p. 1158.

[4] "NASA's Exploration Systems Architecture Study: Final Report," NASA, TM 2005-214062, Nov. 2005, pp. 228, 241.

[5] Brown, C. D., *Spacecraft Mission Design*, AIAA Education Series, AIAA, Washington, D.C., 1992.

[6] Sumrall, J. P., "Ares V Overview," *Ares V Solar System Science Workshop*, 16 April 2008.

[7] Meeus, J., *Astronomical Algorithms*, Willmann–Bell, Richmond, VA, 1991, Appendix II.

[8] Orloff, R. W., and Harland, D. M., *Apollo: The Definitive Sourcebook*, Books In Space Exploration, Springer–Praxis, New York, 2006, p. 581.

I. Boyd
Associate Editor